



NLR-TP-2000-355

**Design guidelines for the prevention
of skin-stiffener debonding in
composite aircraft panels**

J.C.F.N. van Rijn

This report is based on a presentation held at the 15th Technical Conference of the American Society for Composites, College Station, Texas, USA, 2000.

The contents of this report may be cited on condition that full credit is given to NLR and the author.

Division:	Structures and Materials
Issued:	14 August 2001
Classification of title:	Unclassified



Contents

ABSTRACT	3
INTRODUCTION	3
MODEL DEVELOPMENT	5
Model assumptions	5
Basic equations	6
Model results	7
NUMERICAL RESULTS	8
Influence of Skin and Flange Laminates	8
Discussion of Numerical Results	9
CONCLUSIONS	10
REFERENCES	10
 3 Figures	
 APPENDIX A: CALCULATION OF LAMINATE STIFFNESSES	 10

Design Guidelines for the Prevention of Skin-Stiffener Debonding in Composite Aircraft Panels

Joost C.F.N. van Rijn

ABSTRACT

In numerous tests it was established that, in the post-buckling regime, failure of a composite stiffened panel is often induced by the failure of a skin-stiffener interface. The local curvature of the skin induces peel loading at the stiffener flange that results in separation of the skin and the stiffener.

On the basis of experimental research at NLR a failure criterion was proposed for specimens tested in a novel seven-point bending test. A further evaluation of the results is given in the present paper.

The analysis has resulted in the identification of a minimum set of dimensionless parameters, which determine the failure load. The influence of variation in the skin and flange thickness on the failure moment is shown. Moreover, using the analytical framework the correspondence between four- and seven-point bending results noted before was shown to be co-incidental. The methodology presented in this paper can be incorporated in design optimisation tools, which may result in more optimal designs.

INTRODUCTION

Composite materials have become serious candidates for primary structural components of transport aircraft because of potential weight savings. Stiffened panels may be used in these components as primary load-carrying mechanisms. In numerous tests it was established that, in the post-buckling regime, failure of a composite stiffened panel is often induced by the separation failure of a skin-stiffener interface. The local curvature of the skin induces peel loading at the stiffener flange that results in separation of the skin and the stiffener.

Earlier, experimental research at NLR was performed on strip specimens loaded in four-point bending [1]. Evaluation of the results led to the conclusion that specimen failure was governed by the characteristics of the skin and was triggered by stresses concentrated at the edges of the specimen. The influence of the flange lay-up was found to be only marginal. In a follow-on programme four-point bending tests were performed on specimens with three different widths [2]. Findings of the earlier research were largely confirmed. Moreover, the failure moment per unit width was found to increase with an increase in specimen width, which was considered to be undesirable. Based on this conclusion a reconsideration of the coupon-type test was made [2].

A novel seven-point bending test rig was designed and manufactured. In this test configuration, the bending deformation forced onto the specimen was such that failure of the specimen did not initiate at the edges of the specimen. The failure occurred in the

adhesive layer between the flange and the skin, which is in accordance with the failure location found in panels with skin-stiffener interface failure [3]. A new failure criterion was proposed for the specimens tested in seven-point bending. This failure criterion was used to also interpret the results of the four-point bending tests on 100 mm wide specimens. A remarkable similarity between the results of both test methods was established, even though the behaviour and failure characteristics for both test methods were very different. A further evaluation of these results is given in the present paper.

Firstly, the criterion for the failure of the bond layer, as proposed in [2], will be given. Then, a model that uses the proposed criterion will be presented. Subsequently, an evaluation of the results will be given and the influence of variation in the skin and flange thickness on the failure moment is shown. Finally, conclusions reached and recommendations for future work are presented.

CRITERION FOR FAILURE OF THE BOND LAYER

It can be postulated that the running loads transferred through the bond layer govern failure. The running loads transferred through the bond layer are derived from the running loads in the flange through the loads and moments equilibria, as is indicated in Figure 1.c.

The deformation of the flange was obtained from finite element analyses of the seven-point bending test configuration. The flange strains and curvatures were extrapolated to the edge of the flange. These flange strains and curvatures were used as input in the laminate analysis programme LAP to obtain running loads and moments [4]. The shear load F_B and the moment M_B transferred through the bond layer at failure as calculated

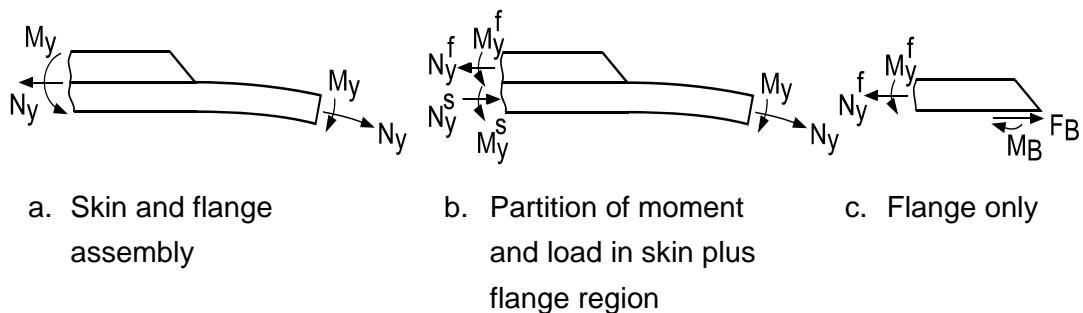


Figure 1 Load and moment equilibria for flange edge

for the specimens tested in seven-point bending are given in Figure 2. The ratio between the shear load and the moment transferred through the bond layer primarily depends on the flange thickness.

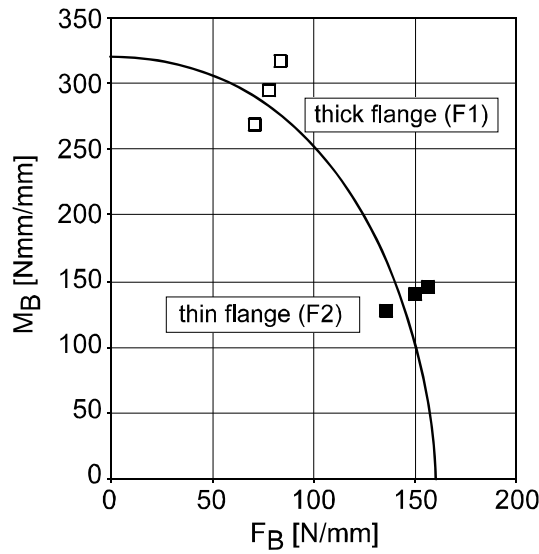


Figure 2 Shear load F_B and moment M_B transferred through the bond layer at failure

A quadratic failure criterion using the bond shear load and the bond moment is postulated

$$\sqrt{\left(\frac{M_B}{M_B^{crit}}\right)^2 + \left(\frac{F_B}{F_B^{crit}}\right)^2} = 1 \quad (1)$$

where F_B^{crit} and M_B^{crit} are the critical values for the shear load and the moment.

This failure criterion is depicted in Figure 2 using values of 160 N/mm and 320 Nmm/mm for F_B^{crit} and M_B^{crit} respectively.

MODEL DEVELOPMENT

Model assumptions

The failure criterion that was derived on the basis of the seven-point bending test results only depends on the running loads in the flange perpendicular to the stringer direction. The running loads can be calculated from the strains and the curvatures in the skin. The following assumptions are used:

- The classical laminate theory is applicable, equations are given in [5].
- The flange and skin laminates are symmetric and balanced.
- The contribution of the bond layer to the stiffness is negligible.
- The deformation in the stringer direction is constant over the region considered.
- A shear strain γ_{xy} , and a shear curvature κ_{xy} are not present.
- The load and moment perpendicular to the stringer direction in the skin are in equilibrium with the load and moment perpendicular to the stringer direction in the combined skin and flange.



The relevant equilibrium conditions are depicted in Figure 1, which shows cross sections of the flange edge perpendicular to the stringer direction. The equilibrium condition is shown in Figure 1.a. The partition of the load and moment in the combined skin and flange into the loads and moments in the flange and the skin is shown in Figure 1.b. The isolation of the flange by introduction of a shear load and a moment in the bond layer is shown in Figure 1.c.

So, as input for the model the following parameters are required:

- skin strains and curvatures ε_x^s , ε_y^s , κ_x^s , and κ_y^s ,
- the A and D matrices of the skin and the flange and
- the thicknesses of the skin, bond layer and flange.

Output are the strain and curvature components ε_y^{sf} and κ_y^{sf} for the skin plus flange region. From these the strain and curvature components ε_y^f and κ_y^f for the flange are calculated, from these the normal load N_y^f and the moment M_y^f in the flange and from these the shear load F_B and the moment M_B transferred through the bond layer.

Basic equations

The load and moment perpendicular to the stringer direction, N_y and M_y , are given by

$$\begin{aligned} N_y^r &= A_{12}^r \cdot \varepsilon_x^r + A_{22}^r \cdot \varepsilon_y^r + B_{12}^r \cdot \kappa_x^s + B_{22}^r \cdot \kappa_y^r \\ M_y^r &= B_{12}^r \cdot \varepsilon_x^r + B_{22}^r \cdot \varepsilon_y^r + D_{12}^r \cdot \kappa_x^s + D_{22}^r \cdot \kappa_y^r \end{aligned} \quad (2)$$

where the superscript r is an indication of the region that is equal to s for the skin region, sf for the skin plus flange region and f for the flange-only region; A_{12} , A_{22} , B_{12} , B_{22} , D_{12} , D_{22} are components of the relevant A, B and D matrices (N.B. for the flange and the skin region the components of B matrix are zero but for the skin plus flange region these components may have a value); ε_x , ε_y , κ_x , κ_y are the strain and curvature components.

Several of the strain and curvature components in a region depend on the strain and curvature components in another region:

$$\begin{aligned} \varepsilon_x^{sf} &= \varepsilon_x^s + \left(\frac{t^a + t^f}{2} \right) \cdot \kappa_x^s \\ \varepsilon_x^f &= \varepsilon_x^s + \left(\frac{t^s}{2} + t^a + \frac{t^f}{2} \right) \cdot \kappa_x^s \\ \varepsilon_y^f &= \varepsilon_y^{sf} + \left(\frac{t^s + t^a}{2} \right) \cdot \kappa_y^{sf} \\ \kappa_y^f &= \kappa_y^{sf} \end{aligned} \quad (3)$$

where t^s , t^a , and t^f are the thicknesses of the skin, the adhesive and the flange respectively.

The components of the A, B and D matrices of the skin plus flange region are functions of the components of the A and D matrices of the flange and the skin:

$$\begin{aligned}
 A_{ij}^{sf} &= A_{ij}^s + A_{ij}^f \\
 B_{ij}^{sf} &= -\left(\frac{t^a + t^f}{2}\right) \cdot A_{ij}^s + \left(\frac{t^s + t^a}{2}\right) \cdot A_{ij}^f \\
 D_{ij}^{sf} &= D_{ij}^s + \left(\frac{t^a + t^f}{2}\right)^2 \cdot A_{ij}^s + D_{ij}^f + \left(\frac{t^s + t^a}{2}\right)^2 \cdot A_{ij}^f
 \end{aligned} \tag{4}$$

where the index ij is equal to 12 or 22.

The load and moment equilibrium as depicted in Figure 1.a gives the following relation:

$$N_y^{sf} = N_y^s \qquad M_y^{sf} = M_y^s - \left(\frac{t^a + t^f}{2}\right) \cdot N_y^f \tag{5}$$

The load and moment equilibrium of the flange-only region as depicted in Figure 1.c renders the shear load and moment in the bond layer:

$$F_B = N_y^f \qquad M_B = M_y^f + \frac{t^f}{2} \cdot N_y^f \tag{6}$$

Model results

The equations given in 2, 3 and 4 are substituted in the equations given in 5. The 2 resulting coupled linear equations are solved to render the strain and curvature components ε_y^{sf} and κ_y^{sf} . After extensive manipulation the following equations evolved:

$$\begin{bmatrix} \varepsilon_y^{sf} \\ \kappa_y^{sf} \end{bmatrix} = \frac{1}{(1 + A_1) \cdot (1 + D_1) + (t_1)^2 \cdot A_1} \cdot \bar{R} \cdot \begin{bmatrix} \varepsilon_x^s \\ \varepsilon_y^s \\ \kappa_x^s \\ \kappa_y^s \end{bmatrix} \tag{7}$$

The components of the 2 by 4 matrix R are:

$$\begin{aligned}
 R_{11} &= -A_2 \cdot (1 + D_1 + t_1 \cdot t_2) \\
 R_{12} &= 1 + D_1 - A_1 \cdot t_1 \cdot (t_1 - t_2) \\
 R_{13} &= -d^s \cdot [A_2 \cdot t_1 \cdot (1 + D_1 + t_1 \cdot t_2) + D_2 \cdot (t_2 + A_1 \cdot (t_2 - t_1))] \\
 R_{14} &= d^s \cdot (t_2 + A_1 \cdot (t_2 - t_1)) \\
 R_{21} &= -A_2 \cdot \frac{t_1}{d^s} \\
 R_{22} &= -A_1 \cdot \frac{t_1}{d^s} \\
 R_{23} &= -A_2 \cdot (t_1)^2 - D_2 \cdot (1 + A_1) \\
 R_{24} &= 1 + A_1
 \end{aligned} \tag{8}$$

The dimensionless parameters A_1 , A_2 , D_1 , D_2 , t_1 , and t_2 , and the parameter d^s with dimension [m] are defined as follows:

$$\begin{aligned}
 A_1 &= \frac{A_{22}^f}{A_{22}^s} & A_2 &= \frac{A_{12}^f}{A_{22}^s} & D_1 &= \frac{D_{22}^f}{D_{22}^s} & D_2 &= \frac{D_{12}^f}{D_{22}^s} & (9) \\
 t_1 &= \frac{t^s + 2 \cdot t^a + t^f}{2 \cdot d^s} & t_2 &= \frac{t^a + t^f}{2 \cdot d^s} & d^s &= \sqrt{\frac{D_{22}^s}{A_{22}^s}}
 \end{aligned}$$

NUMERICAL RESULTS

Influence of Skin and Flange Laminates

The methodology outlined above was used to calculate the shear load F_B and the moment M_B transferred through the bond layer for the case of a prescribed curvature κ_y^s with the other strains and curvature equal to zero. The calculated shear load F_B and the moment M_B were substituted in the failure criterion, equation (1).

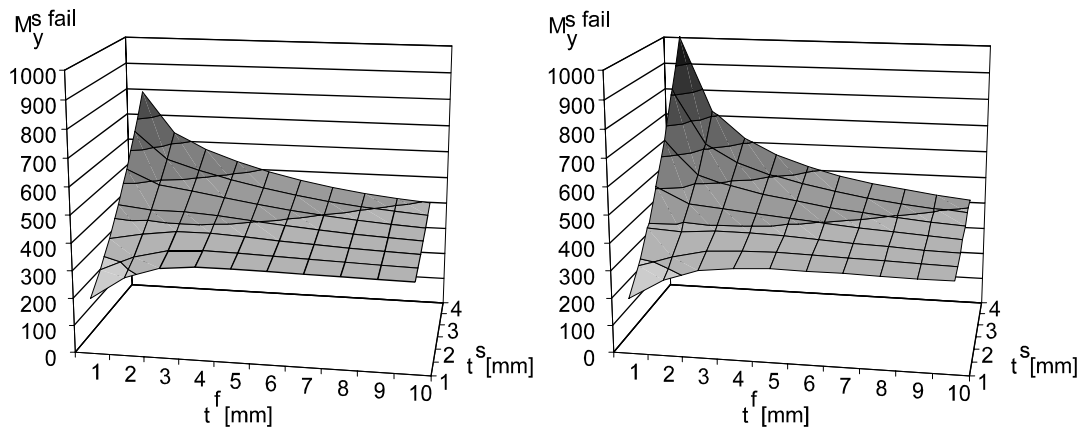
The applied moment follows from:

$$M_y^s = \kappa_y^s \cdot D_{22}^s \quad (10)$$

As all calculations are based on linear equations, the moment to be applied to the skin in order to cause failure of the skin-stiffener interface is proportional to the applied moment and inversely proportional to the failure criterion value:

$$M_y^{s, failure} = \frac{\kappa_y^s \cdot D_{22}^s}{\sqrt{\left(\frac{M_B}{M_B^{crit}}\right)^2 + \left(\frac{F_B}{F_B^{crit}}\right)^2}} \quad (11)$$

The moment to be applied to the skin in order to cause failure was calculated for a series of skin thicknesses and a series of flange thicknesses with both skin and flange laminates having a quasi-isotropic lay-up. The A and D matrices of the skin and flange



- a. Quasi-isotropic lay-up for skin and flange laminates b. Quasi-isotropic lay-up for skin and hard lay-up for flange laminate

Figure 3 Moment to be applied to the skin in order to cause failure of the skin-stiffener interface, as function of the skin and flange thickness



laminates were calculated using the equations given in APPENDIX A. The results of these calculations are shown in Figure 3.a. As can be seen, optimum flange thickness exists for the skins with a thickness of 1 to 2 mm. This optimum flange thickness was approximately 5 and 3 mm respectively. The failure moments for an optimum flange thickness were respectively 67 percent and 11 percent higher than failure moments for the minimum flange thickness of 1 mm. For thicker skins, a thicker flange would give a lower failure moment.

The moment to be applied to the skin in order to cause failure was also calculated for a series of skin thicknesses and a series of flange thicknesses with skin laminates having a quasi-isotropic lay-up and flange laminates having a hard (55% 0°, 36 % ±45°, 9% 90°) lay-up. The 0° direction is parallel to the stringer direction. The results of these calculations are shown in Figure 3.b. For the 1 mm thick skin, the relation between the flange thickness and the failure moment was almost the same as in figure 3.a. The variation in failure moment for the 2 mm thick skin with a variation in flange thickness was only minor. The difference in behaviour in comparison to quasi-isotropic flange laminates might be attributable to the lower transverse stiffness of the laminates with a hard lay-up.

Discussion of Numerical Results

The postulated criterion should be verified with experiments on specifically designed configurations. The failure envelope is premature since only two points are available for the construction of the envelope. More experiments are needed to cover the range for the ratio between the shear load and the moment transferred through the bond layer more fully.

The dependence of the failure moment on the flange thickness for thinner skins is remarkable. This result is important, as the occurrence post-buckling of skins would be most likely for structures with thinner skins. Of course, due precaution should be exercised as the experimental basis for the methodology is still rather limited.

Clearly, a dependence of the failure moment on the flange thickness exists. This dependence was not found with the four-point bending tests [1, 2]. The four-point bending tests also gave different failure characteristics compared to the seven-point bending tests. On the basis of these observations it can be concluded that the correspondence between the four- and seven-point bending results depended on the configurations chosen to evaluate the methods and was therefore co-incidental.

The failure criterion derived on the basis of the seven-point bending test results is incorporated in the design optimisation code PANOPT. PANOPT was developed at the National Aerospace Laboratory NLR for the design of stiffened composite panels for primary aircraft structures with buckling and post-buckling constraints [6]. Previously, a constraint was placed on the thickness of the stiffener flange in order to prevent failure of the skin-stiffener interface in the post-buckling regime. Based on the findings in the present paper, it can be concluded that this approach might even be non-conservative for panels with thin skins. The new approach will give a more optimal design.



CONCLUSIONS

A novel bending test configuration was developed and a failure criterion postulated.

This criterion must still be verified with experiments on specifically designed configurations. More experiments are needed to cover the range for the ratio between the shear load and the moment transferred through the bond layer more fully.

The dependence of the failure moment on the flange thickness for thinner skins is remarkable. This result is important, as post-buckling of skins would be most likely for structures with thinner skins.

The correspondence between the four- and seven-point bending results, as noted earlier, was shown to be co-incidental.

The failure criterion derived on the basis of the seven-point bending test results is incorporated in a design optimisation code. For panels with a skin thickness of more than 2 mm the new approach is likely to give a more optimal design.

REFERENCES

1. van Rijn, J.C.F.N., 1998, *Failure criterion for the skin-stiffener interface in composite aircraft panels*, National Aerospace Laboratory NLR Technical Publication 98264
2. van Rijn, J.C.F.N., 2000, *A seven-point bending test to determine the strength of the skin-stiffener interface in composite aircraft panels*, National Aerospace Laboratory NLR Technical Publication 2000-044
3. Bowen, R., and E. Greenhalgh, 2000, *Characterisation of skin/stiffener and skin/spar type joints in composite structures*, , DERA Report No. DERA/MSS/MSM2A/TR000804
4. LAP, 1996, *Laminate Analysis Programme, User Guide*, Anaglyph Ltd, London
5. Tsai, S.W., and H.T. Hahn, 1980, *Introduction to composite materials*, Technomic Publishing Co., Inc.
6. Arendsen, P., H.G.J.S. Thuis and J.F.M. Wiggenraad, 1994, *Optimization of composite stiffened panels with post-buckling constraints*, National Aerospace Laboratory NLR Technical Publication 94083

APPENDIX A: CALCULATION OF LAMINATE STIFFNESSES

A method to create a series of laminates that are constructed by stacking symmetric and balanced base laminates. It was established that the following relations hold for the components of the A and D matrices:

$$A_{ij}^r = A_{ij}^{r*} \cdot t^r \qquad D_{ij}^r = D_{ij}^{r*} \cdot t^r + \frac{A_{ij}^{r*}}{12} \cdot (t^r)^3 \qquad (A.1)$$

where the index ij is equal to 12 or 22 and the superscript r is an indication of the laminate that is equal to s for the skin and f for the flange.



The coefficients $A_{ij}^{r^*}$ and $D_{ij}^{r^*}$ follow from

$$A_{ij}^{r^*} = \frac{A_{ij}^b}{t^b} \quad D_{ij}^{r^*} = \frac{D_{ij}^b}{t^b} - \frac{A_{ij}^b}{12} \cdot t^b \quad (\text{A.2})$$

where the superscript b indicates base laminate parameters.